

1 Article

2 **Preparation and characterization of an electrospun**
3 **PLA-cyclodextrins composite for simultaneous high-**
4 **efficiency PM and VOC removal**5 Silvia Palmieri ^{1*}, Mattia Pierpaoli ^{2*}, Luca Riderelli ³, Sheng Qi ⁴ and Maria Letizia Ruello ^{1,*}6 ¹ Department of Materials, Environmental Sciences and Urban Planning-(SIMAU), Università Politecnica
7 delle Marche, Ancona, Italy; s.palmieri@pm.univpm.it (SP), m.l.ruello@univpm.it (MLR)8 ² Department of Metrology and Optoelectronics, Faculty of Electronics, Telecommunication and Informatics,
9 Gdańsk University of Technology, Gdańsk, Poland; mattia.pierpaoli@pg.edu.pl10 ³ Professional Engineer, Via Bartolini 13/A, 60027 Osimo, Ancona, Italy; lucariderelli@gmail.com11 ⁴ School of Pharmacy, University of East Anglia, Norwich Research Park, Norwich, UK NR4 7TJ

12 * Correspondence: (SP) s.palmieri@pm.univpm.it; (MLR) m.l.ruello@univpm.it; (MP)

13 mattia.pierpaoli@pg.edu.pl;

14 Received: date; Accepted: date; Published: date

15 **Abstract:** Electrospinning is known to be a facile and effective technique to fabricate fibres of a
16 controlled diameter-distribution. Among a multitude of polymers available for the purpose, the
17 attention should be addressed to the environmentally compatible ones, with a special focus on
18 sustainability. Polylactic acid (PLA) is a widespread, non-toxic, originated from renewable sources,
19 polymer and it can degrade into innocuous products. While the production of fibrous membranes
20 is attractive for airborne particles filtration applications, their impact on the removal of gaseous
21 compounds is generally neglected. In this study, electrospun PLA-based nanofibers were
22 functionalized with cyclodextrins, because of their characteristic hydrophobic central cavity and a
23 hydrophilic outer surface, in order to provide adsorptive properties to the composite. The aim of
24 this work is to investigate a hybrid composite, from renewable sources, for the combined filtration
25 of particulate matter (PM) and adsorption of volatile organic compounds (VOCs). Results show how
26 their inclusion into the polymer strongly affects the fibre morphology, while their attachment onto
27 the fibre surface only positively affects the filtration efficiency.

28 **Keywords:** Polylactic Acid; electrospinning; nanofibers; air filtration

29

30 **1. Introduction**

31 Air filtration is the most effective and widespread method to remove particulate matters (PM)
32 from the air stream. Air filter material and morphology play a major role in the process efficiency and
33 sustainability. Electrospinning is a versatile method commonly used to manufacture polymer
34 nanofiber[1].

35 The concept of green electrospinning has been introduced with the aim of reducing the toxicity and
36 environmental problem related to the use of potentially hazardous-organic solvents for the
37 electrospinning of natural or synthetic polymers [2]. While this aspect is of primary importance in
38 regenerative medicine, in which the absence of impurity is compulsory, when the electrospun fibre
39 mat is used in much larger extends for air filtration applications, the focus should be addressed to
40 the polymer type as well, favouring polymer from renewable sources, easily disposable, having a low
41 environmental impact. Since indoor air quality has become not only an issue but also a need, due to
42 the risks people are exposed to and in connection with the amount of time spent in confined
43 environment, both at work and home [3]. In addition to common pollutants of outdoor air, it must

44 be considered other unusual sources like furniture, copiers, and air fresheners, and so on. Also,
 45 people themselves are a source of potentially harmful agents i.e. spread as indoor bioaerosol.

46 Electrospinning of functional polymeric nanofibers has attracted considerable attention in the past
 47 decade due to the simplicity of the process and the enhanced properties associated with the size of
 48 the fibres [4–6]. One potential application for electrospun nanofibers is in the field of filtration where
 49 the nanowebs can provide separation of tiny particles due to the different interception mechanism.

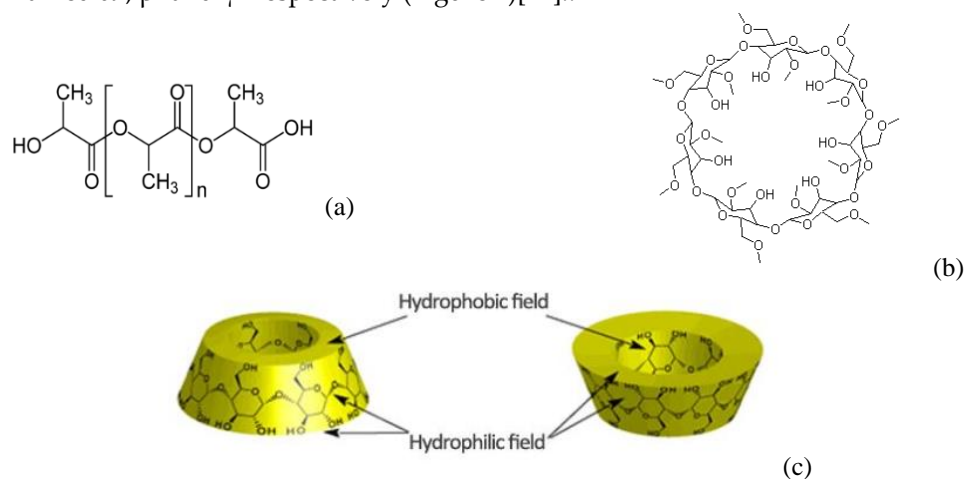
50 PLA is a thermoplastic aliphatic polyester derived from renewable resources, so it has been
 51 chosen for its environmentally friendly properties as its biodegradability.

52 The fabrication of PLA electrospun nanofibers has been widely investigated by many authors because
 53 of the great availability, the production from renewable sources, the non-toxicity, and the known
 54 biodegradability[7–9]

55 Casasola and co-workers [10] investigated the effect of different solvents on the fibre morphology. In
 56 particular, they found that the acetone-based binary solvent system was the most effective to produce
 57 electrospinnable nanofibers.

58 In the study of Wang et al. [11], porous bead-on-string poly(lactic acid) (PLA) nanofibrous
 59 membranes (NMs) were fabricated to investigate the filtration performance by measuring the
 60 penetration of sodium chloride (NaCl) aerosol particles. Without further modification, a high
 61 filtration efficiency was obtained, by controlling the solvent solution.

62 Cyclodextrins (CDs) are conical, truncated macrocycles, consist of six, seven, and eight α -d-glucose
 63 units, and named α -, β - and γ - respectively (Figure 1)[12]..



64 **Figure 1.** a) PLA chemical structure; (b) CyD chemical structure; (c) representation of CyD
 65 structure.

66 They are environmentally friendly and deserve attention for their valuable properties thanks to their
 67 chemical structure. In fact, they are commonly applied in different fields: from pharmaceutical
 68 carriers [12–14] to the use as nano-sponges in water treatments [13,15].. Cyclodextrins can form
 69 complexes of inclusion with numerous poorly soluble molecules, this is the reason why they are
 70 commonly used in pharmaceutical chemistry as carriers. Hydrophobic molecules are maintained in
 71 the cavity of the cyclodextrin with the outer surface of the complex maintaining its hydrophilic
 72 characteristics [12,16]. Wen and colleagues [17] incorporated cinnamon essential oil/beta-
 73 cyclodextrin into PLA nanofilm to give better antimicrobial activity compared to conventional
 74 nanofilm, prolong the shelf life of food, as an active food packaging. Similarly, in the works of Aytac
 75 et al.[18], beta-cyclodextrin is used for the stabilization of active compounds in the production of
 76 functional electrospun PLA nanofibers incorporating naturally occurring antioxidant compound [18].
 77 Taking advantages of their molecular structure to block lipophilic molecules, such as volatile organic
 78 compounds (VOCs), another use for cyclodextrins has been proposed [20,21] for air pollution control
 79 applications. While cyclodextrins have already been used for the removal of organic pollutants in
 80 wastewater [15,21,22], they have not been used in much lesser extends for air treatments and removal
 81 of PMs and VOCs.

82 In this study, for the first time, an electrospun PLA/cyclodextrin composite has been produced
83 and characterized for the joint filtration of particulate matter (PM) and enhanced adsorption of VOCs.
84 The electrospun nanocomposite exhibits not only excellent PM filtration efficiency, but the presence
85 of CyD provides to the composite material a two-fold improved adsorption ability measured in terms
86 of toluene removal.

87 2. Materials and Methods

88 2.1 Material

89 Dichloromethane (DCM) and N,N-Dimethylformamide (DMF) of analytical grade were
90 purchased from Sigma-Aldrich. PLA has been used to prepare a polymeric solution of 8% w/V
91 solubilized in DCM/DMF (80:20). The electrospinning setup consists of a house-made syringe pump,
92 which needle is connected to the high potential (16kV). The flow rate was 0.5 ml/h and the
93 needle/collector distance equal to 10cm. Nanofibers are electrospun over a PLA-based 3D printed
94 support, placed on a grounded aluminium foil (See supplementary materials).

95 All the prepared composites were electrospun over 3D-printed support (1mm thick) with large
96 voids (60% fill). Pictures of the substrate and 3d printing parameters are reported in the supporting
97 materials. Both support and nanofibers produced with electrospinning technique are made by the
98 same polymer to improve the affinity, permitting a better adhesion between them [23]. [12,19] In this
99 study B-methyl-cyclodextrins (Carbosynth) have been also used either in association with fibers as
100 such (in powder) or solubilized in methanol (Sigma-Aldrich) and electrospun. Cyclodextrins were
101 both incorporated in the PLA solution, both dispersed on the PLA surface. Three different
102 configurations were studied: a) PLA solubilized in the solvent and then electrospun (PLA); b) a three
103 levels configuration where a layer of cyclodextrins in powder was placed in the middle of a bi-layer
104 of electrospun PLA (PLA/CyD); c) Cyclodextrins were solubilized in few droplets of methanol and
105 added in the same solution of PLA then electrospun (PLA+CyD).

106 2.2. Characterization

107 All the specimens have been analyzed with a ZEISS Scanning electron microscope for the
108 characterization of the morphological aspect and to evaluate the interaction between PLA fibres and
109 CyD.

110 The samples were analyzed by using a Perkin-Elmer Spectrum GX1 spectrometer (PerkinElmer,
111 Inc, Waltham, MA, USA) equipped with U-ATR accessory for the analysis of solid samples in
112 reflectance mode. On each sample, 5 spectra were acquired in the range between 4000-500 cm^{-1} , with
113 a spectral resolution of 4 cm^{-1} and recording 64 scans. A background adsorption spectrum was
114 recorded before each acquisition. Raw FTIR spectra were converted in absorbance, interpolated in
115 the 1800-500 cm^{-1} spectral range and vector normalized in the same interval. An automatic baseline
116 correction algorithm was used in all spectra to avoid errors due to baseline shifts. Atmospheric
117 compensation was also performed. The average absorbance spectra of all samples were also
118 calculated, and they were fitted in the 1800-800 cm^{-1} upon two-points baseline correction and vector
119 normalization (Grams AI 9.1 software, Galactic Industries, Inc., Salem, NH). A Gaussian algorithm
120 was adopted. For each underlying band, the positions in terms of wavenumbers, height and
121 integrated area were calculated. Spectrum 5.3.1 (Perkin-Elmer) was used as the operating software.

122 2.3. PM generation and efficiency tests

123 In the filtration efficiency tests, PM particles were generated by burning incense in an 82 l box.
124 The smoke PM particles have a wide size distribution from <300 nm to 4 μm , with the majority of
125 particles being <1 μm . The so-generated particle stream was controlled by dilution with air. PM
126 particle number concentration was measured with a GRIMM 1.108 particle counter and the removal
127 efficiency was calculated by comparing the number concentration before and after filtration, while
128 the pressure drop in the filter medium was measured by a differential pressure meter (Honeywell

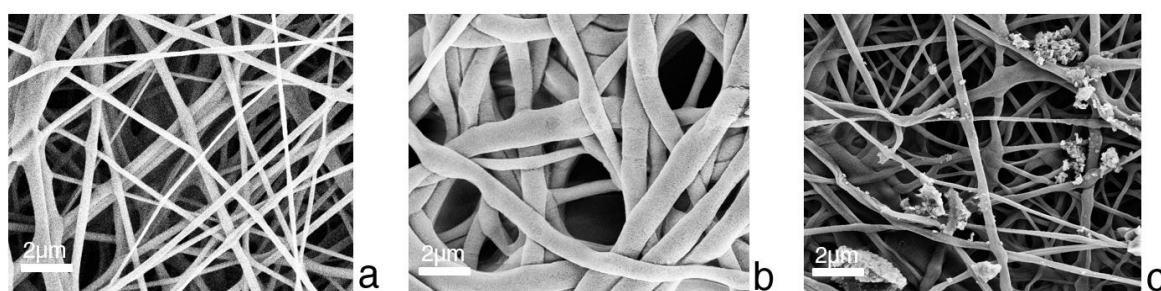
129 160 PC). The wind velocity, measured in absence of the filter with a hot-wire anemometer, was equal
 130 to 1.4 m s^{-1} .

131 VOC removal tests were performed in the same box environments, with the injection of $100 \mu\text{l}$
 132 Toluene, and the test started when its full vaporization occurred. VOC concentration was measured
 133 with a ppbRAE 3000 with 1-min sample time, and the VOC removal efficiency was calculated,
 134 likewise for PM, by comparing the number concentration before and after filtration. All the tests were
 135 performed at the temperature of $27 \pm 2^\circ\text{C}$ and RH equal to $50 \pm 10\%$.

136 **3. Results**

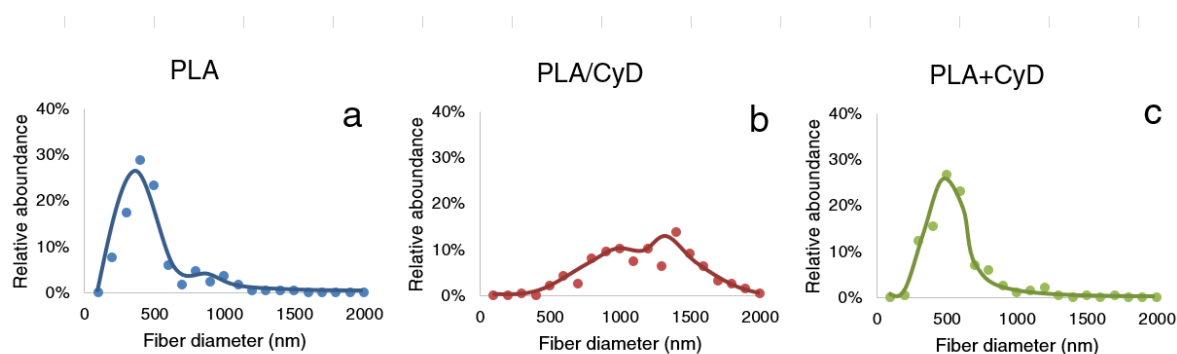
137 *3.1. Electrospun nanofiber morphology*

138 Figure 2 reports SEM pictures of the three reference filter composites, with only PLA (Figure 2a),
 139 with the addition of CyD in bulk solution (Figure 2b) and over the PLA fibre (Figure 2c). The median
 140 diameters of the PLA-based fibres composites electrospun from the solutions were determined to be
 141 350, 990, and 530 nm, respectively (Figure 3.)



142

143 **Figure 2.** SEM pictures of (a) PLA, (b) PLA/CyD and (c) PLA+CyD electrospun nanofibers.



144

145 **Figure 3.** Fiber diameter distribution for (a) PLA, (b) PLA/CyD and (c) PLA+CyD
 146 electrospun nanofibers.

147 The Fibrous filter pressure drops were measured at low face velocity. Pressure drop and outlet
 148 air velocity, as a function of the fibre type and fibre loading values, have been reported in Table 1.

149 **Table 1.** Composition and characterization of the electrospun filter media.

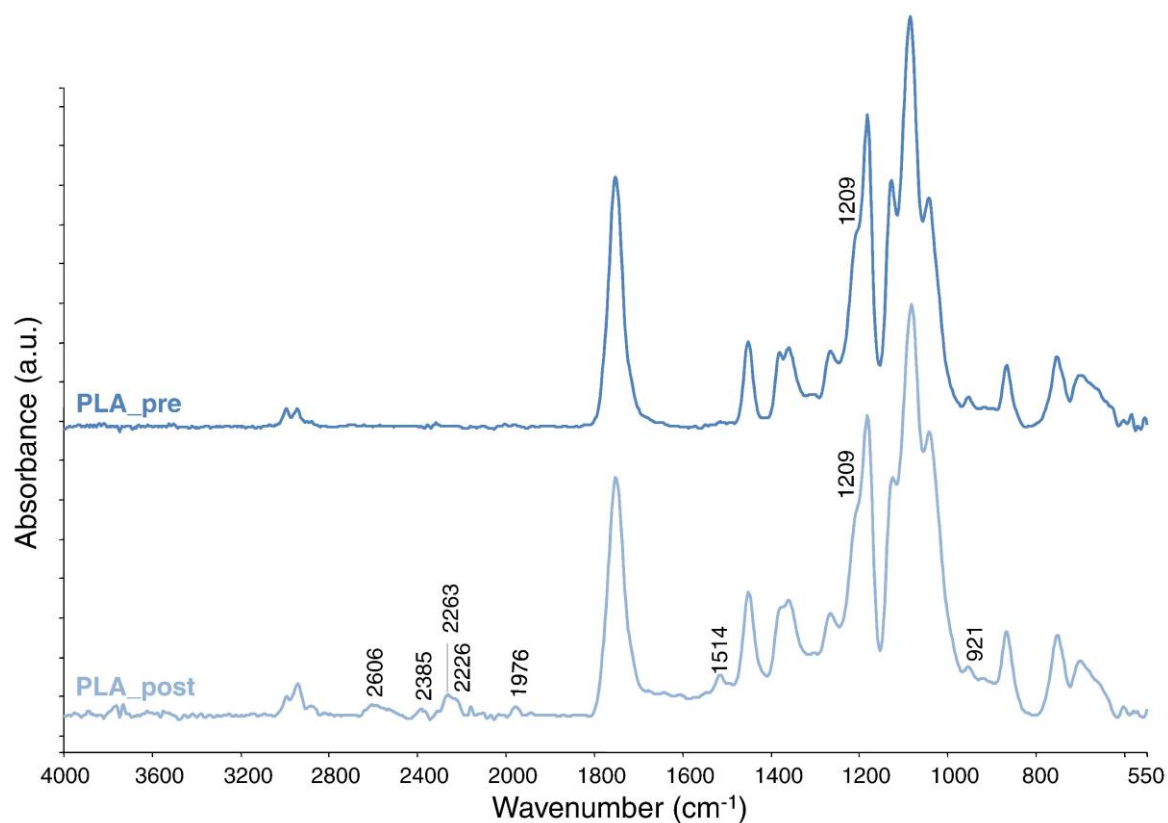
Filter	solution		CyD	v_{outlet} (m/s)	ΔP (Pa)	Filter loading (mg/cm^2)
	PLA	CyD				
PLA	100%	0	-	0.25	24.4	1.43
PLA/CyD	98.5%	1.5%	-	0.41	33.9	2.47
PLA+CyD	100%	-	1.5%	0.24	29.9	4.05

150

151 Starting with these data, analyses on images were carried out to find out correlations with
152 dimensions and morphology of the fibres. Observing the three filters (Figure 2), cyclodextrins
153 influence the result of electrospinning and the overall measured pressure drop (Table 1, ΔP 24.4, 33.9,
154 and 29.9 respectively). Filters PLA/CyD show apparently more bulky fibres (Table 1, Filter loading
155 (mg/cm²), 1.43, 2.47, and 4.05) fibres than the ones of PLA and PLA+CyD filters. This comparison
156 justifies a higher drop pressure for this filter (33.9 Pa). Furthermore, crossing fibres enhance thickness
157 determining a probably augmented capacity of sieving phenomena. PLA mix differentiates itself
158 from PLA/CyD and PLA+CyD only for the addition of CyD.

159 3.2. FTIR Spectroscopy

160 FTIR spectroscopy was used to determine the interaction between both PLA and CyD and the
161 composite and pollutants[24]. Obviously, due to a large number of functional groups present due not
162 only to the enormous variability of the compounds present in the polluting source used for the tests
163 but also to the polymeric ones of the filter, it is not possible to identify with certainty the filtered
164 molecules. It is instead possible to determine by the difference the presence or absence of pollutants.
165 In this regard, it was necessary to outline a spectroscopic profile of the materials used to make the
166 filter itself, to also study the interaction between the polymer and the CyDs. The enormous variety of
167 compounds present in the polluting source does not always and unequivocally allow to have the
168 same peaks, so it is necessary to search for the traces of pollutant by evaluating the shifts and all the
169 variations between the different peaks. Figure 4 reports a comparison between the untested and the
170 tested PLA filter (without CyDs). The spectra of the pristine filter show the main peaks attributable
171 to the PLA: at 2997-2944cm⁻¹ there are the symmetrical and the asymmetrical stretching of CH₂ and
172 CH₃; the characteristic peak of a carbonyl group is at 1753 cm⁻¹; at 1453 cm⁻¹ there is the methyl in α
173 position respect to the carbonyl group and in the region of 1380-1000cm⁻¹ the bending signals of CH₂
174 and CH₃.



175

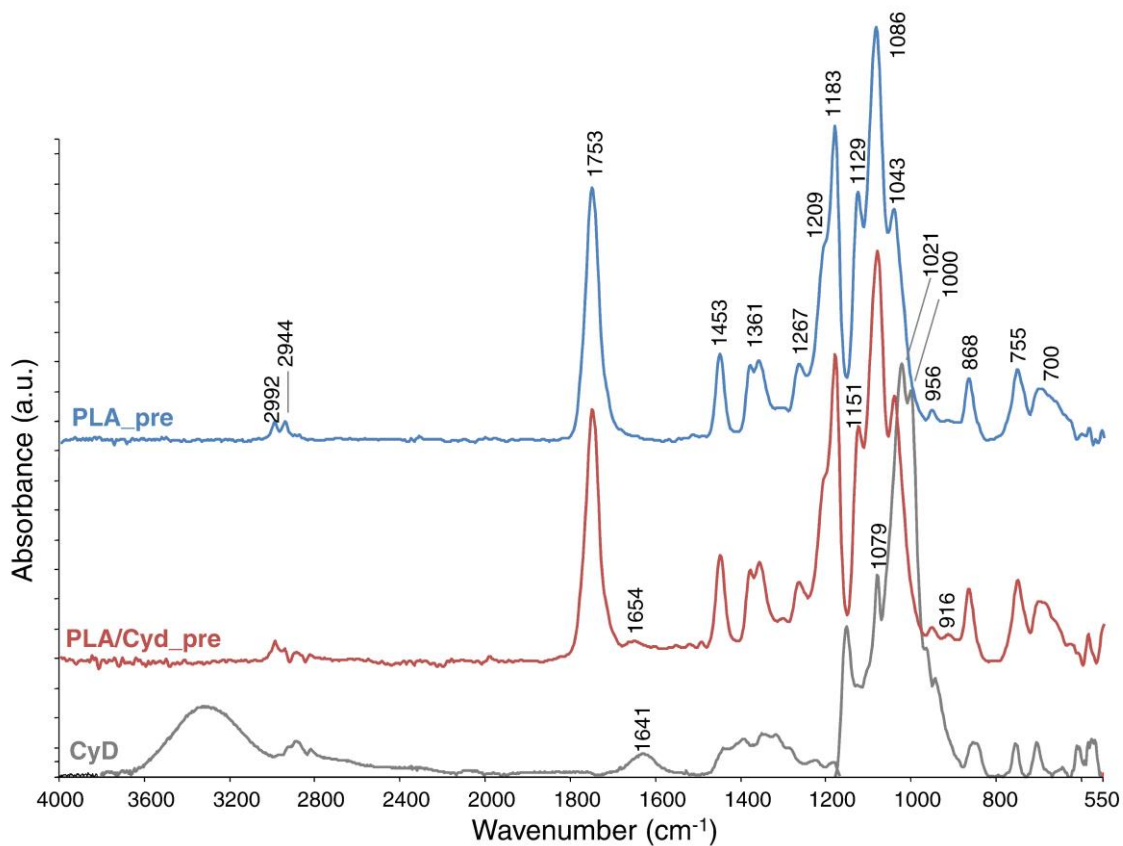
176

Figure 4. FTIR spectra of tested and untested PLA filters.

177 In the other spectra, the different peaks caused by the interaction of the polymer with pollutants
178 can be easily individuated: at 1644, 1541, 1514, 1301 cm^{-1} and 953 cm^{-1} . Confronting the peak of the
179 carbonyl group at 1753 cm^{-1} of the no tested filter with the same peak of the other samples reports a
180 shift caused by the interaction between the polymer and the pollutant. It is possible to suppose the
181 presence of nitro groups, reported by the peaks in the range of 1541 cm^{-1} and 1514 cm^{-1} ; the presence
182 of aldehydes because of the shift at 1754 cm^{-1} and the peak at 1644 cm^{-1} ; and a carbon-nitrogen bound,
183 due to the presence of a peak at 1301 cm^{-1} .

184 The peak at 1514 cm^{-1} is very sharp respect to the other spectres, it is reasonable to assume that
185 this is due to the concentration of pollutant adsorbed. A peak at 1514 cm^{-1} can be attributed or to a NO
186 or a CN group. Moreover, it presents a series of peaks at 2601, 2385, 2263 and 1976 cm^{-1} . Usually, in
187 this range, there are signals from inorganic contaminants as, for example, thiocyanate. Considering
188 the CN at 1514 cm^{-1} at the level of bands' ratio, the signal of the triple bonds is present at 2200 cm^{-1} ; the
189 -SH group is at 2600 cm^{-1} and the signal of SCN is at 2100 cm^{-1} . The peak at 1209 cm^{-1} is different in
190 terms of height, therefore the concentration of the respective group increases after the filtration, so a
191 pollutant containing the same group is attached to the filter. Lastly, at 921 cm^{-1} a new peak appears,
192 which was absent in the pristine filter, so it is may be relative to the deposited pollutant.

193 For what concerns the filters made with the addition of cyclodextrins (PLA/CyD and PLA+CyD),
194 it was important to determinate the possible interaction between the polymer and the CyD molecules,
195 because during the electrospinning process these two compounds could interact causing the presence
196 of new peaks independent from the wavelengths of the single compounds. It was necessary to
197 determine the shifts and the new peaks on a no tested filter, not only to have a reference standard for
198 the identification of the pollutant, but also to estimate the level of the bond between the two
199 compounds. In Figure 5 is reported the spectra of the filter untested, made by adding CyD not only
200 in the between of two layers of the polymer (PLA+CyD), but also in the polymer solution (PLA/CyD).
201 Analysing this spectrum, it is immediately notable the absence of the characteristic peak of the
202 hydroxylic group at 3400 cm^{-1} , because a large quantity of these groups is bonded with PLA in
203 hydrogen bonds; but the peak at 1654 cm^{-1} indicates that there are still some free. All the values at
204 1000, 1021, 1077 and 1151 cm^{-1} are shifted to 1040, 1082, 1124 and 1182 cm^{-1} because of the hydrogen
205 bonds between the two compounds. Also, the peak at 850 cm^{-1} , typical of C-C bond, is shifted to 916
206 cm^{-1} . The shift of the signal can be caused not only by the formation of new bonds but also by the sum
207 of two different signals in the same region.



208

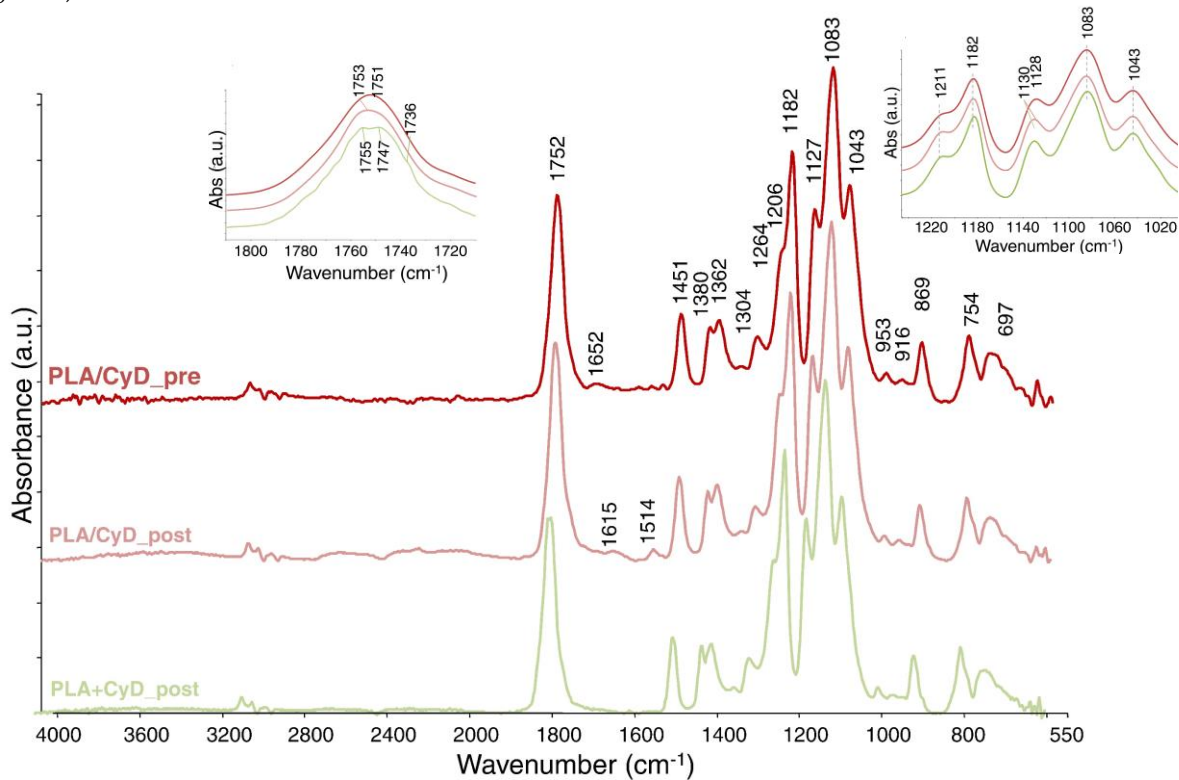
209

Figure 5. Typical spectra of the filter containing PLA and CyDs.

210

After the reference spectra for the filters containing CyD, also the tested spectra were examined (Figure 6).

211



212

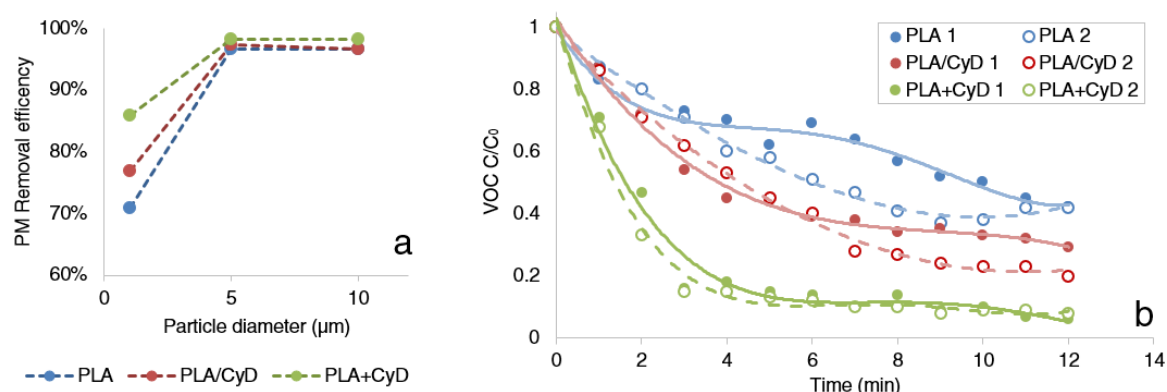
213

Figure 6. Comparison between all the filters containing cyclodextrins.

214 In these samples the presence of contaminates is represented by two main behaviours: the most
 215 important is the split of the carbonyl peak and its slightly shift; the other change is the shift of all the
 216 characteristic bands in the range from 1220 cm^{-1} to 1000 cm^{-1} . The split of the carbonyl group can
 217 indicate the presence of another molecule with a similar configuration (for instance it can be an
 218 aldehyde or a ketone). Moreover, these kinds of pollutants may cause also the shoulder at 1736 cm^{-1} .
 219 Other particular peaks are present at 3377 cm^{-1} for PLA/CyD: the peak at 3377 cm^{-1} can be attributed to
 220 a compound with NH group, seeing as there are also peaks at 1615 and 1514 cm^{-1} , which usually
 221 indicate the presence of NH_2 and of a carbon bonded to nitrogen. The series of peaks in the range
 222 from 870 to 700 cm^{-1} are typical of CH groups: in these cases, they are different from the reference
 223 because of their shape and their shift, indicating the presence of another compound different from
 224 Cyclodextrins or PLA.

225 3.3. PM and VOC removal tests

226 The PM_{10} , $\text{PM}_{2.5}$ and PM_{10} removal by different fibrous filters is shown in Figure 7(a). From the
 227 PM efficiency removal comparison, it is possible to observe that the PLA+CyD has the highest
 228 removal of both smaller particles, while all the different samples exhibit an efficiency higher than
 229 97% for particles having diameter greater than $2.5\text{ }\mu\text{m}$.



230

231 **Figure 7.** (a) PM removal efficiency and (b) normalized VOC concentration versus time by
 232 the different fibrous filters.

233 The characteristic conical configuration of cyclodextrins [12] is suitable for the formation of
 234 complexes of inclusion through non-covalent interactions: in fact, hydrophobic molecules are
 235 maintained in the cavity, blocking their passage through the filter.

236 This mechanism of filtration should be added, according to classical filtration theory, to the other
 237 five mechanism effects to catch particles (interception, inertial, diffusion, gravity, and static electricity
 238 effect) [25] to catch also other smaller molecules as VOCs. In this way, CyD plays a role both in
 239 affecting the fibre morphology, resulting in thicker fibres and reduced cavities, and, actively, as
 240 surface centres for the capture of PM and VOCs, due to their dual hydrophilic/hydrophobic nature.
 241 The presence of CyD molecules at the surface of the fibres has a large influence on the molecular
 242 filtration capability [26]. The presence of more CyDs on the surface of the fibres implies a higher
 243 availability of sites for the bond with the pollutants, so it is reasonable to assume that higher
 244 concentration of CyDs are beneficial for the overall filtration efficiency. Nevertheless, the superficial
 245 availability of adsorption centres will affect also the blocking capacity of PMs and the resulting
 246 pressure drop. For all these reasons, the amount of CyDs must be enough to be bonded to the polymer
 247 and sufficient to have the possibility to create hydrogen bond with the pollutants.

248 During the electrospinning, CyD molecules could phase separate from PLA matrix and formed
 249 heterogeneous dispersion during solvent evaporation in the electrospinning process: this is likely
 250 because CyD has a hydrophilic characteristic and PLA is a hydrophobic polymer [26]. A heterogenic
 251 solution may cause a not homogeneous presence of CyDs on the fibre surface, causing a not
 252 homogenous filter.

253 VOCs removal is shown in Figure 7(b). In this graph, it is possible to compare the three different
 254 tested filters in two subsequent situations. These tests were conducted injecting Toluene in the box.
 255 The first curve is about the behaviour with 100 µl of Toluene (in Figure 7(b) labelled with 1). After
 256 about 30 minutes and as curves reach a plateau or their background concentration, the second
 257 injection of Toluene was carried out (20 µl). This second injection (in Figure 7(b) labelled with 2) is
 258 sufficient to obtain an initial concentration of Toluene comparable to the first one. The purpose of this
 259 method consists in investigating repeatability of tests and in the first evaluation of the durability of
 260 filters. As it was expected, filters with cyclodextrins allow quicker removal of VOCs, referred to PLA
 261 only fibres. Besides, it can be observed that the two normalized curves are almost overlapped,
 262 highlighting a factual constant behaviour, for two subsequent tests at high concentration at least.

263 The presence of cyclodextrins in filters points out an increased capacity in the removal of VOCs.
 264 This condition suggests that VOCs removal tests highlight the contribution of the CyD on adsorption.
 265 Thus, the CyD can empower the removal of VOCs in two different ways. It is probable that in
 266 PLA/CyD filters VOCs are removed when CyD have their hole available. In PLA+CyD filters, VOCs
 267 are removed when they collide with CyD powder with an enhanced capacity of removal because of
 268 entire exposure to air, with a higher number of available sites.

269 A non-exhaustive comparison of the obtained results with the one reported in the literature is
 270 reported in Table 2.

271 *Table 2 – Comparison of the obtained filtration results with the one reported in the literature*

Electrospun Polymer	Efficiency	Comments	Ref
PLA	99.997% (165.3 Pa)	Small fibre diameter and the presence of additional mesopores on the beads were conducive to the capture and adsorption of particulates.	[11]
PLA/TiO ₂	99.996% (128.7 Pa)	Relative humidity of 45% and face velocity of 5.3 cm/s and a high antibacterial activity of 99.5%	[27]
PLA/CNPs	98.99% (147.60 Pa)	Air flow rate of 14 cm/s. PLA/chitosan fibres show a highly porous structure	[28]
PVA/CNCs	99.1% (91 Pa)	Tests with PM2.5 and airflow velocity of 0.2 m/s	[29]
Hierarchical structured nano-sized/porous PLA	99.999% (93.3 Pa)	PLA-N/PLA-P double-layer structured membrane with a mass ratio of 1/5. Face velocity of 5.3 cm/s	[30]
PAN	>99% (27 Pa)	Nanobeads are useful for reducing the packing density and the pressure drop through the filter. Ultrafine nanofibers guarantee the PM removal efficiency. Airflow rate of 4.2 cm/s	[31]
PLA/CyD	> 98% (30Pa)		<i>This study</i>

272 DMAC: dimethylacetamide; CNPs: Chitosan nanoparticles; CNCs: cellulose nanocrystals

273 4. Conclusions

274 The addition of CyD both in bulk and powder determines an increase of removal efficiency of
 275 VOCs and PM1 size fraction, due to two different effects: the CyD in bulk affect the PLA fibres
 276 morphology, while the superficially deposited CyD directly affect the removal of the VOC. Efficiency
 277 tests highlight enhanced VOC removal efficiency in PLA/CyD and PLA+CyD filters; the FTIR analysis
 278 confirms that in filters containing CyDs the traces of the interaction between the pollutants and the
 279 filter are more evident, showing shifted and larger bands, split and sharper peaks. Further studies
 280 will involve the investigation of the VOC type on the adsorption property, with the simultaneous
 281 addition of functional composites and the aim of synthesizing such composite from starch-food

282 wastes. The use of CyDs from food wastes in air filtration systems will improve their positive
283 environmental impact in a circular economy perspective for being used in air filtration applications.
284

285 **Author Contributions:** Conceptualization, Silvia Palmieri, Mattia Pierpaoli, Luca Riderelli and Sheng
286 Qi; Data curation, Mattia Pierpaoli, Silvia Palmieri, Luca Riderelli; Formal analysis, Silvia Palmieri,
287 Luca Riderelli and Maria Letizia Ruello; Investigation, Silvia Palmieri, Luca Riderelli and Sheng Qi;
288 Methodology, Silvia Palmieri, Mattia Pierpaoli, Luca Riderelli and Sheng Qi; Project administration,
289 Maria Letizia Ruello; Resources, Sheng Qi and Maria Letizia Ruello; Supervision, Maria Letizia
290 Ruello; Writing – original draft, Silvia Palmieri and Luca Riderelli; Writing – review & editing, Mattia
291 Pierpaoli, and Maria Letizia Ruello.

292 **Funding:** This research received no external funding

293 **Acknowledgments:** We would like to thank: Total Corbion PLA for providing the PLA and Dr.
294 Simona Sabbatini from the SIMAU (Department of Materials, Environmental Sciences and Urban
295 Planning) for the FTIR measurements.

296 **Conflicts of Interest:** The authors declare no conflict of interest.

297 References

- 298 1. Reneker, D.H.; Yarin, A.L.; Zussman, E.; Xu, H. ELECTROSPINNING OF NANOFIBERS
299 FROM POLYMER SOLUTIONS. *Polymer (Guildf)*. **2007**, doi:10.1016/S0065-2156(06)41002-4.
- 300 2. Krishnan, R.; Sundarrajan, S.; Ramakrishna, S. Green Processing of Nanofibers for
301 Regenerative Medicine. *Macromol. Mater. Eng.* **2012**, *298*, n/a-n/a,
302 doi:10.1002/mame.201200323.
- 303 3. Pierpaoli, M.; Ruello, M.L. IAQ : a bibliometric study. **2018**, 1–20.
- 304 4. Yang, F.; Murugan, R.; Wang, S.; Ramakrishna, S. Electrospinning of nano/micro scale poly(l-
305 lactic acid) aligned fibers and their potential in neural tissue engineering. *Biomaterials* **2005**,
306 *26*, 2603–2610, doi:10.1016/j.biomaterials.2004.06.051.
- 307 5. Mohammadian, M.; Haghi, A.K. Systematic parameter study for nano-fiber fabrication via
308 electrospinning process. *Bulg. Chem. Commun.* **2014**, *46*, 545–555,
309 doi:10.1016/j.polymer.2005.05.068.
- 310 6. Chakraborty, S.; Liao, I.C.; Adler, A.; Leong, K.W. Electrohydrodynamics: A facile technique
311 to fabricate drug delivery systems. *Adv. Drug Deliv. Rev.* **2009**, *61*, 1043–1054,
312 doi:10.1016/j.addr.2009.07.013.
- 313 7. You, Y.; Won, S.; Jin, S.; Ho, W. Thermal interfiber bonding of electrospun poly (L -lactic acid
314) nanofibers. **2006**, *60*, 1331–1333, doi:10.1016/j.matlet.2005.11.022.
- 315 8. Park, J.; Lee, I. Controlled release of ketoprofen from electrospun porous polylactic acid (PLA
316) nanofibers. **2011**, 1287–1291, doi:10.1007/s10965-010-9531-0.
- 317 9. Li, Y.; Lim, C.T.; Kotaki, M. Study on structural and mechanical properties of porous PLA
318 nanofibers electrospun by channel-based electrospinning system. *Polym. (United Kingdom)*
319 **2015**, *56*, 572–580, doi:10.1016/j.polymer.2014.10.073.
- 320 10. Casasola, R.; Thomas, N.L.; Trybala, A.; Georgiadou, S. Electrospun poly lactic acid (PLA)
321 fibres: Effect of different solvent systems on fibre morphology and diameter. *Polym. (United*
322 *Kingdom)* **2014**, *55*, 4728–4737, doi:10.1016/j.polymer.2014.06.032.
- 323 11. Wang, Z.; Zhao, C.; Pan, Z. Porous bead-on-string poly(lactic acid) fibrous membranes for air
324 filtration. *J. Colloid Interface Sci.* **2015**, *441*, 121–129, doi:10.1016/j.jcis.2014.11.041.
- 325 12. Aulton, M.E.; Taylor, K.M.G. *Tecnologie Farmaceutiche-Progettazione e allestimento dei medicinali*;

- 326 Edra, Ed.; London, 2015; ISBN 9780702042904.
- 327 13. Sliwa, W.; Girek, T. *Cyclodextrins. Properties and Application*; Wiley-VCH, Ed.; 2017; ISBN
328 9783527339808.
- 329 14. Kayaci, F.; Umu, O.C.O.; Tekinay, T.; Uyar, T. Antibacterial Electrospun Poly(lactic acid)
330 (PLA) Nanofibrous Webs Incorporating Triclosan/Cyclodextrin Inclusion Complexes. *J. Agric.*
331 *Food Chem.* **2013**, doi:10.1021/jf400440b.
- 332 15. Arkas, M.; Allabashi, R.; Tsiourvas, D.; Mattausch, E.M.; Perfler, R. Organic/inorganic hybrid
333 filters based on dendritic and cyclodextrin “nanosponges” for the removal of organic
334 pollutants from water. *Environ. Sci. Technol.* **2006**, *40*, 2771–2777, doi:10.1021/es052290v.
- 335 16. Favier, I.M.; Baudelet, D.; Fourmentin, S. VOC trapping by new crosslinked cyclodextrin
336 polymers. In Proceedings of the Journal of Inclusion Phenomena and Macrocyclic Chemistry;
337 Springer, 2011; Vol. 69, pp. 433–437.
- 338 17. Wen, P.; Zhu, D.H.; Feng, K.; Liu, F.J.; Lou, W.Y.; Li, N.; Zong, M.H.; Wu, H. Fabrication of
339 electrospun polylactic acid nanofilm incorporating cinnamon essential oil/ β -cyclodextrin
340 inclusion complex for antimicrobial packaging. *Food Chem.* **2016**, *196*, 996–1004,
341 doi:10.1016/j.foodchem.2015.10.043.
- 342 18. Aytac, Z.; Kusku, S.I.; Durgun, E.; Uyar, T. Encapsulation of gallic acid/cyclodextrin inclusion
343 complex in electrospun polylactic acid nanofibers: Release behavior and antioxidant activity
344 of gallic acid. *Mater. Sci. Eng. C* **2016**, *63*, 231–239, doi:10.1016/j.msec.2016.02.063.
- 345 19. Loftsson, T.; Duchêne, D. Cyclodextrins and their pharmaceutical applications. *Int. J. Pharm.*
346 **2007**, *329*, 1–11, doi:10.1016/j.ijpharm.2006.10.044.
- 347 20. Butterfield, M.T.; Agbaria, R.A.; Warner, I.M. Extraction of volatile PAHs from air by use of
348 solid cyclodextrin. *Anal. Chem.* **1996**, *68*, 1187–1190, doi:10.1021/ac9510144.
- 349 21. Crini, G.; Peindy, H.N.; Gimbert, F.; Robert, C. Removal of C.I. Basic Green 4 (Malachite
350 Green) from aqueous solutions by adsorption using cyclodextrin-based adsorbent: Kinetic
351 and equilibrium studies. *Sep. Purif. Technol.* **2007**, *53*, 97–110, doi:10.1016/j.seppur.2006.06.018.
- 352 22. Alsbaiee, A.; Smith, B.J.; Xiao, L.; Ling, Y.; Helbling, D.E.; Dichtel, W.R. Rapid removal of
353 organic micropollutants from water by a porous β -cyclodextrin polymer. *Nature* **2016**, *529*,
354 190–194, doi:10.1038/nature16185.
- 355 23. Pierpaoli, M.; Riderelli, L.; Palmieri, S.; Fava, G.; Ruello, M.L. Transparent electrospun PLA-
356 nanofibers on 3D-printed honeycomb for a high-efficient air filtration . **2017**, 2–3.
- 357 24. Medhurst, L.J. FTIR Determination of Pollutants in Automobile Exhaust : An Environmental
358 Chemistry Experiment Comparing Cold-Start and Warm-Engine Conditions. **2005**, 82.
- 359 25. Qin, X.; Wang, S. Filtration Properties of Electrospinning Nanofibers. **2006**,
360 doi:10.1002/app.24361.
- 361 26. Uyar, T.; Havelund, R.; Hacaloglu, J.; Besenbacher, K.F.; Kingshott, P. Cyclodextrins :
362 Comparison of Molecular Filter Performance. *ACS Nano* **2010**, *4*, 5121–5130.
- 363 27. A Novel Hierarchical Structured Poly(lactic acid)/Titania Fibrous Membrane with Excellent
364 Antibacterial Activity and Air Filtration Performance., doi:10.1155/2016/6272983.
- 365 28. Li, H.; Wang, Z.; Zhang, H.; Pan, Z. Nanoporous PLA/(Chitosan Nanoparticle) Composite
366 Fibrous Membranes with Excellent Air Filtration and Antibacterial Performance. *Polymers*
367 *(Basel)*. **2018**, *10*, 1085, doi:10.3390/polym10101085.
- 368 29. Zhang, Q.; Li, Q.; Young, T.M.; Harper, D.P.; Wang, S. A Novel Method for Fabricating an

- 369 Electrospun Poly(Vinyl Alcohol)/Cellulose Nanocrystals Composite Nanofibrous Filter with
370 Low Air Resistance for High-Efficiency Filtration of Particulate Matter. *ACS Sustain. Chem.*
371 *Eng.* **2019**, *7*, 8706–8714, doi:10.1021/acssuschemeng.9b00605.
- 372 30. Wang, Z.; Pan, Z. Preparation of hierarchical structured nano-sized/porous poly(lactic acid)
373 composite fibrous membranes for air filtration. *Appl. Surf. Sci.* **2015**, *356*, 1168–1179,
374 doi:10.1016/j.apsusc.2015.08.211.
- 375 31. Huang, J.J.; Tian, Y.; Wang, R.; Tian, M.; Liao, Y. Fabrication of bead-on-string
376 polyacrylonitrile nanofibrous air filters with superior filtration efficiency and ultralow
377 pressure drop. *Sep. Purif. Technol.* **2020**, *237*, 116377, doi:10.1016/j.seppur.2019.116377.
- 378 32. Pierpaoli, M.; Zheng, X.; Bondarenko, V.; Fava, G.; Ruello, M.L. Paving the Path to A
379 Sustainable and Efficient SiO₂ / TiO₂ Photocatalytic Composite. **2019**, 1–14.
- 380



© 2020 by the authors. Submitted for possible open access publication under the terms and conditions of the Creative Commons Attribution (CC BY) license (<http://creativecommons.org/licenses/by/4.0/>).